The Improvement Effect of Sodium Ferulate on the Formation of Pulmonary Fibrosis in Silicosis Mice Through the Neutrophil Alkaline Phosphatase 3 (NALP3)/Transforming Growth Factor-β1 (TGF-β1)/α-Smooth Muscle Actin (α-SMA) Pathway

Authors' Contribution:
Study Design A
Data Collection B
Statistical Analysis C
Data Interpretation D
Manuscript Preparation E
Literature Search F
Funds Collection G

AE Jingyin Han
BCD Yangmin Jia
BCD Shujuan Wang
BCD Xiaoyu Gan

Department of Occupational Disease, Hangzhou Red Cross Hospital, Hangzhou, Zhejiang, P.R. China

Corresponding Author: Jingyin Han, e-mail: hanjyin_hjyin@163.com
Source of support: This work was supported by Zhejiang Medical and Health Science and Technology Plan Project (2020KY739)

Background: Pneumoconiosis is a chronic progressive fibrotic interstitial pneumonia for which the pathogenesis and treatment remain unclear. Previous studies showed that sodium ferulate (SF) may have a therapeutic effect, and this study explored the mechanism underlying SF-related improvement.

Material/Methods: In this study, a silicosis mouse model and primary cultured mouse lung fibroblasts were established. Hematoxylin-eosin staining, western blot analysis, quantitative real-time polymerase chain reaction, and Masson staining were used to observe the lung injury, expression of vimentin, and the degree of pulmonary fibrosis. The extracted lung fibroblasts were identified by immunofluorescence. The expression of fibrosis-related genes encoding transforming growth factor-β1 (TGF-β1), neutrophil alkaline phosphatase 3 (NALP3), collagen-1, α-smooth muscle actin (α-SMA), and phosphorylated p38 (p-p38) and p38 proteins were detected by western blot. The effects of SF and the TGF-β pathway agonist SRI-011381 on cell proliferation and the expression of fibrosis-related protein in mouse lung fibroblasts were measured by Cell Counting Kit-8, immunofluorescence, and western blot as needed.

Results: SF reduced the lung lesions in silicosis mice and inhibited the expression of vimentin and fibrosis-related genes, while having no effect on body weight. Vimentin expression was positive in the extracted cells. In vitro experiments showed that SF inhibited the proliferation of lung fibroblasts and the expression of fibrosis-related proteins. In addition, SF partly reversed the opposite regulatory effect of SRI-011381 on lung fibroblasts.

Conclusions: SF inhibited lung injury and fibrosis in silicosis mice through the NALP3/TGF-β1/α-SMA pathway.

Keywords: Cell Proliferation • Silicosis • Transforming Growth Factors

Full-text PDF: https://www.medscimonit.com/abstract/index/idArt/927978

📄 3783   📊 1   📈 4   📖 45

Background

Pulmonary fibrosis is a major pathological change of pneumoconiosis, which is confined to the lungs and mostly occurs in middle-aged and elderly men. The main symptoms are dyspnea, restricted ventilation dysfunction, gas exchange disorder, and cough [1-3]. During the formation of silicosis, many cytokines can stimulate the proliferation of human fibroblasts and an abnormal deposition of extracellular matrix, which constitute an important link in the formation and progression of silicosis fibrosis [4,5].

Many cytokines activate the signal transduction pathways of target cells via their receptors [6]. In recent years, the neutrophil alkaline phosphatase 3 (NALP3) inflammatory complex has been found to play an important role in the process of pulmonary fibrosis [7]. Studies have shown that transforming growth factor-1 (TGF-β1), α-smooth muscle actin (α-SMA), NALP3, collagen-1, and phosphorylated p38 (p-p38) play key roles in the occurrence and development of pulmonary fibrosis [8-11]. TGF-β1 can promote the abnormal proliferation of lung fibroblasts and stimulate fibroblasts to synthesize extracellular matrix, which then accumulates excessively between the lung interstitium and alveoli [12]. TGF-β1 can also induce the expression of protease inhibitors, eventually leading to further abnormal accumulation of extracellular matrix and fiber formation [13]. α-SMA is the main phenotypic marker of myofibroblasts, and changes in its level predict whether myofibroblasts are activated [14].

At present, Western medicine mainly treats pulmonary fibrosis with glucocorticoids and immunosuppressive drugs, which have therapeutic effects but cannot significantly improve patients' quality of life [15]. Therefore, the formation and development of pulmonary fibrosis could theoretically be inhibited by finding the key pathogenic factors for pulmonary fibrosis, interfering with the pathogenic factors from the perspective of molecular biology, and using drugs against its biological effects to prevent fibroblast proliferation and abnormal deposition of the extracellular matrix.

With the rapidly increasing interest in traditional Chinese medicine (TCM) in recent years, scientists have discovered that TCM has a certain curative effect on pulmonary fibrosis by activating blood and removing stasis. The research shows that a DangGui BuXue decoction can improve liver fibrosis in experimental animals and can be clinically used to treat coal workers' pneumoconiosis and significantly improve cardiopulmonary function [16,17]. Sodium ferulate (SF) is the main effective component of *Angelica sinensis*, which has antioxidant activity and an anti-atherosclerosis effect and causes relaxation of vascular smooth muscle and inhibition of platelet aggregation [18]. Research shows that SF can inhibit liver fibrosis and renal interstitial fibrosis in rats [19,20].

In this study, we constructed a silicosis mouse model and an experimental method of lung fibroblast culture in vitro to observe the impact of SF on the NALP3/TGF-β1/α-SMA pathway in the formation of silicosis fibrosis.

Material and Methods

Ethics Statement

All animal experiments were performed in accordance with the guidelines of the China Council on Animal Care and Use. This study was approved by the Committee of Experimental Animals of Zhejiang Chinese Medical University (No. YF2018020424). Every effort was made to minimize pain and discomfort in animals. The animal experiments were performed in Zhejiang Chinese Medical University.

Preparation and Grouping of Silicosis Model Mice

The specific pathogen-free Kunming mice (Beijing Vital River Laboratory Animal Technology Co., Ltd.) used in this study were healthy males with a body weight of about 20-22 g. The animal license number was scxk (Beijing) 2015-0001. For the construction of the silicosis model, mice were intraperitoneally anesthetized with 0.2 mL of 1% pentobarbital sodium (P3761, Sigma-Aldrich, USA), and a silicon dioxide (SiO$_2$, S5631, Sigma, USA) suspension was infused into their bronchi at a dosage of 200 mg/kg for 4 weeks [21]. Control mice received an equal volume of physiological saline (PS). A total of 40 mice were divided into 4 groups, with 10 mice in each group. All mice were weighed every 2 days for 8 weeks.

In the control group, mice were subjected to bronchial infusion of 0.1 mL of sterile PS for 8 weeks (Control 8w). In the Control 4w+SF 4w group, mice were subjected to bronchial infusion of 0.1 mL sterile PS for 4 weeks, followed by perfusion of 100 mg/kg of SF (3-methoxy-4-hydroxy-cinnamate sodium, C$_{10}$H$_9$NaO$_4$, B20008, Yuan ye, Shanghai, China) into the bronchus for the following 4 weeks. In the Model 4w+PS 4w group, after the silicosis model was constructed with bronchial infusion of 0.1 mL SiO$_2$ suspensions for 4 weeks, 0.1 mL of sterile PS was injected for 4 weeks. In the Model 4w+SF 4w group, after the silicosis model was constructed, mice were subjected to bronchial infusion of 100 mg/kg of SF for 4 weeks [22]. All animals were sacrificed by cervical dislocation after the 8-week period ended. The pulmonary tissues from the different groups were collected; part of the pulmonary tissues were collected for pathological observation, and the remaining tissues were prepared for the isolation of lung fibroblasts.

Table 1. Gene sequence primers.

Name	Forward primer (5'-3')	Reverse primer (5'-3')
Vimentin	TGAAGGAAGATGGCTCGT	TCCAGCAGCTTCCTGTAGGT
GAPDH	AGCTTCGGCACATATTTCATCTG	CGTTCACTCCCATGACAAACA

Pathological Observation of Lung Tissue

The right lower lung lobe was routinely retained, washed with phosphate-buffered saline (PBS), and fixed with 10% neutral formaldehyde solution (M004, G fan, Shanghai, China) for 48 h. The right lower lung lobe was routinely dehydrated, embedded in paraffin, and sliced. The slices were mounted on glass slides, which were then placed in an oven at 60°C for 30 min and then immersed in 100% xylene for 10 min twice (xylene I and II). The slides were placed in anhydrous ethanol I and II for 15 min each, followed by 90%, 80%, 70%, and 60% ethanol for 5 min each. The slides were then washed with tap water for 5 min 3 times. Hematoxylin (B25380, Yuan ye) staining was performed for 5-10 min, after which the slides were washed with running water. Next, 1% hydrochloric acid ethanol differentiation solution (R20778, Yuan ye) was used for 1-2 s and sections were hydrated for 15 min, after which they turned blue. Eosin (S26233, Yuan ye) staining was used for 1 min, and the slides were then washed with running water. The sections were dehydrated with 60%, 70%, 80%, and 90% anhydrous ethanol for 5 min each, and anhydrous ethanol I and II for 15 min each. Slides were immersed in xylene I and II for 15 min each to make the slices transparent, and neutral mounting medium was used to seal coverslips over the slices. Histopathological changes were observed under an optical microscope (Olympus D72, Olympus, Tokyo, Japan) with ×100 magnification.

Western Blot

We used a western blot procedure that was slightly modified from a previous report [23]. The total protein in the lung tissue homogenate and lung fibroblasts were extracted with RIPA lysate containing phenylmethylsulfonyl fluoride (R0010, Solarbio, Beijing, China). Protein content was determined by the BCA kit (PC0020, Solarbio). Protein samples were separated by 10% sodium dodecyl sulfate-polyacrylamide gel electrophoresis and transferred to a polyvinylidene difluoride (PVDF) membrane (no. R8BA8116C, Millipore, CA, USA). The PVDF membrane was placed in a petri dish containing 5% skim milk blocking solution and set on a shaker at room temperature for 1 h. The PVDF membrane was incubated with anti-TGF-β1 (1: 1000 dilution, AB92486, Abcam, USA), anti-vimentin (1: 1000 dilution, SAB4503081, Sigma-Aldrich, USA), anti-NALP3 (1: 1000 dilution, 254160, Abbiotec, USA), anti-collagen-1 (1: 1000 dilution, AB34710, Abcam), anti-α-SMA (1: 1000 dilution, bs-10196R-2,

Bioss, China), anti-p-p38 (1: 1000 dilution, AB195049, Abcam), anti-p38 (1: 1000 dilution, AB170099, Abcam), and anti-GAPDH (1: 5000 dilution, AB181602, Abcam) antibodies at 4°C overnight, followed by incubation with goat anti-rabbit secondary antibody (1: 5000 dilution, AB6721, Abcam) at 37°C for 1 h. According to the manufacturer's instructions for ECL Plus hypersensitive luminescent liquid, an appropriate amount of ECL chemiluminescence reagent (SW2010-1, Solarbio) was added. After being placed in the dark for about 3 min, the membranes were developed in a gel imager (12003151, Bio-Rad, Co., Ltd., USA).

Quantitative Real-Time Polymerase Chain Reaction

After total RNA was extracted from lung tissue with an RNA extraction kit (19Ba2706, Mei5, Beijing, China), an RNA reverse transcription kit (19Da3005, Mei5, Beijing, China) was used to reverse transcribe RNA into cDNA. Gene expression was analyzed by real-time fluorescence quantitative polymerase chain reaction (PCR) kit (19Ca0702, Mei5, Beijing, China). The 96-well plate was centrifuged and placed in the PCR instrument (LightCycler480, Roche, Germany). Reaction conditions were pre-denaturation at 94°C for 2 min, denaturation at 94°C for 20 s, annealing at 53°C for 30 s, and extension at 72°C for 40 s, for 45 cycles. The relative expression of the target gene was analyzed by the relative quantitative method ($2^{-\Delta\Delta Ct}$) [24]. Primer sequences (Shanghai General Co., Ltd., China) are shown in **Table 1**.

Masson Staining

Paraffin sections were mounted on glass slides and deparaffinized to water and then washed in tap water and distilled water. The sections were placed in iron hematoxylin staining solution (R20387, Yuan ye) for 5 min for staining of the nuclei and washed with tap water. The slides were then placed in acid ethanol (R20777, Yuan ye) for a few seconds (5-15 s) and washed with tap water. The sections were rinsed with running water for a few minutes until a blue color developed and again washed with tap water. Next, the sections were dyed with ponceau acid fuchsin solution (S31373, Yuan ye) for 5 min and rinsed with distilled water. The slides were then placed in 1% molybdophosphoric acid solution (R20400, Yuan ye, Shanghai, China) for 3 min. After the solution was drained, the sections were treated with 2% glacial acetic acid solution (64-19-17, Sigma, USA) for 30-60 s, stained with bright green

aniline blue solution for 6 min, washed twice with distilled water, and then treated with 2% glacial acetic acid solution for 30-60 s. The sections were dehydrated with 95% ethanol and anhydrous ethanol, and then sealed with toluene-based transparent and neutral mounting medium. The sections were observed under an optical microscope (Olympus D72, Olympus, Tokyo, Japan) with ×100 magnification to determine the degree of pulmonary fibrosis.

Isolation and Culture of Lung Fibroblasts

For further investigation of the effects of SF on pulmonary fibroblasts in vitro, pulmonary fibroblasts were isolated from the pulmonary tissues of the model mice. The tissues were extracted in a sterile environment, rinsed in PBS (SH30256.01B, Hyclone, USA) 3 times, and then cut into 1-mm^3 tissue blocks. After repeated digestion with 0.25% trypsin (Gibco, USA) at 37°C, the histolysate was evenly spread in a 10-cm petri dish. A high-glucose medium containing 10% fetal bovine serum (16000-044, Gibco, USA), penicillin, and streptomycin was added to the petri dish. The cells were cultured in an incubator, and the medium was exchanged every 2-3 days. When the cells reached 80-90% confluence, they were passaged according to the ratio of 1: 3, and the fifth passage cells were taken for experimental study [25]. Pulmonary fibroblasts were identified using anti-vimentin antibody with fluorescent secondary antibodies under a fluorescence microscope (DM2000, Olympus, Tokyo, Japan).

For in vitro experiments, a range of concentrations of SF solution (0.04, 0.1, 0.18 and 0.28 mg/mL) were prepared for the treatment of fibroblasts. A 10 μM SRI-011381 solution was used for the activation of TGF-β1 signaling.

Immunofluorescence

The cells were spread on a glass slide at a density of 1×10^4/mL. After the cells adhered to the surface of the slide and grew to 70% confluence, the cells were starved overnight in a serum-free medium, which was then replaced with serum-free medium containing the corresponding treatment. After incubation in the incubator for 48 h, the culture medium was removed. The cells were then fixed with 4% paraformaldehyde, lysed with 0.1% Triton X-100 (DXT-11332481001, Roche, USA), and covered with 1% bovine serum albumin, to which anti-vimentin primary antibody was added according to the manufacturer's instructions (4828-30-06, Cell Signaling Technology, Danvers, MA, USA), followed by incubation at 37°C for 1 h. After treatment with fluorescent secondary antibodies, 4 ,6-diaminido-2-phenylindole (DAPI, DXT-10236276001, Roche) was added to combine with the nucleus, following Lyu et al [26]. Fluorescence-positive expression changes of cells in each group were observed under a fluorescence microscope

(DM2000, Olympus, Tokyo, Japan) with ×200 magnification, and images were collected.

Bromodeoxyuridine Assay

Bromodeoxyuridine (BrdU) (Sigma-Aldrich) reagent was dissolved in PBS, added to the medium (1: 1000), and incubated 24 h before fixation in 4% paraformaldehyde at 4°C overnight, followed by treatment with 2 N HCl at room temperature and washing with 0.1 M borate buffer (pH 8.0). After being permeabilized in 0.25% Triton X-100 (Sigma-Aldrich) for 1 h, cells were treated with mouse anti-BrdU antibody (Abcam, ab8152, 1: 300) overnight at 4°C. After a wash stage with PBS, cells were incubated with secondary antibodies for 2 h at room temperature. The cell nuclei were then stained with DAPI. Fluorescence-positive expression changes of cells in each group were observed under a fluorescence microscope (DM2000, Olympus) with ×200 magnification.

Enzyme-Linked Immunosorbent Assay

Caspase-1 and interleukin (IL)-1β in culture supernatants were assessed with a mouse IL-1β enzyme-linked immunosorbent assay (ELISA) kit (BD Biosciences, San Diego, CA, USA) and caspase-1 ELISA kit (Antibodies-online GmbH, Aachen, Germany) according to the manufacturers' instructions. Culture medium was centrifuged at 500×g for 5 min, the supernatant was collected, and levels of IL-1β and caspase-1 were measured.

Cell Counting Kit (CCK)-8

Cells were seeded at a density of 5×10^4/mL in 96-well plates (6 multiple wells). After the cells adhered and grew to 70% confluence, they were starved overnight with serum-free medium. The control group, 0.04 mg/mL SF group, 0.1 mg/mL SF group, 0.18 mg/mL SF group, and 0.28 mg/mL SF group were added, and the 96-well plates were cultured in a culture tank for 48 h. Ten microliters of CCK-8 (CK04, Dojindo, Japan) solution was added to each well, and the cells were incubated at 37°C for 1 h. Then the absorbance at 450 nm was determined with a microplate reader (ELX808, BioTek, USA).

Statistical Analysis

The data were analyzed by SPSS 20.0 (IBM, Armonk, NY, USA) software, and the statistical significance of the differences between groups was analyzed by 1-way analysis of variance followed by Dunnett's post hoc test. All data are expressed as mean±standard deviation (SD). $P<0.05$ was considered to indicate a statistical difference.
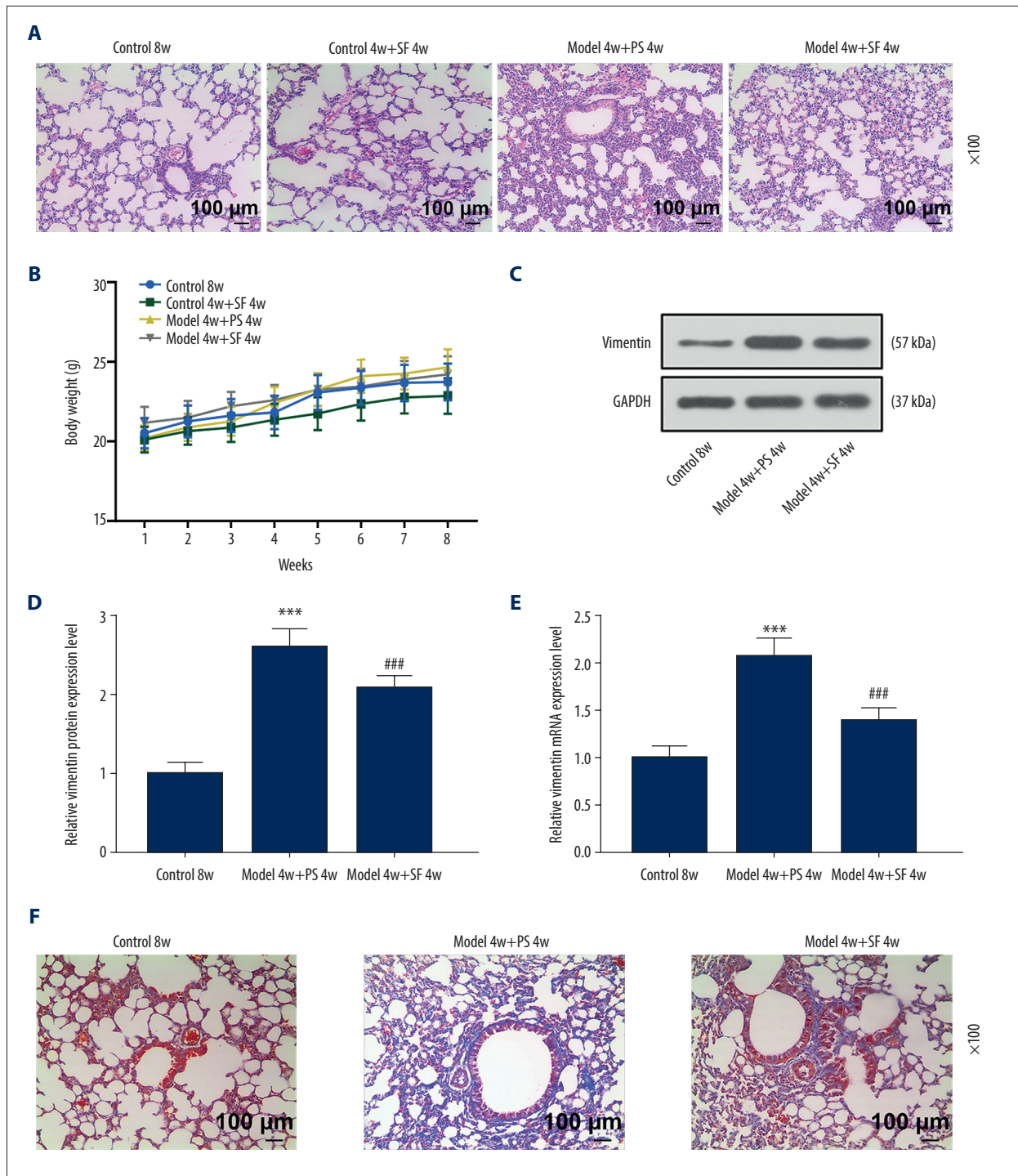
Figure 1. Sodium ferulate (SF) reduced the injury of silicosis mice, specifically lung lesions and fibrosis, by inhibiting vimentin, while having no effect on body weight. (**A**) The effect of SF on lung tissue lesions in the silicosis mice was observed by hematoxylin-eosin staining (magnification×100, n=10, scale bars=100 μm). (**B**) The effect of SF on body weight of silicosis mice (n=10). (**C-E**) The effect of SF on vimentin protein and mRNA expression in silicosis mice was detected by western blot and quantitative real-time polymerase chain reaction (qRT-PCR). Expression levels were normalized with GAPDH. (**F**) The effect of SF on pulmonary fibrosis in silicosis mice (magnification×100, n=10, scale bars=100 μm). All experiments were performed in triplicate, and data are expressed as mean±standard deviation (SD). *** $P<0.001$ vs control 8 weeks; ### $P<0.001$ vs model 4 weeks+physiological saline (PS) 4 weeks.
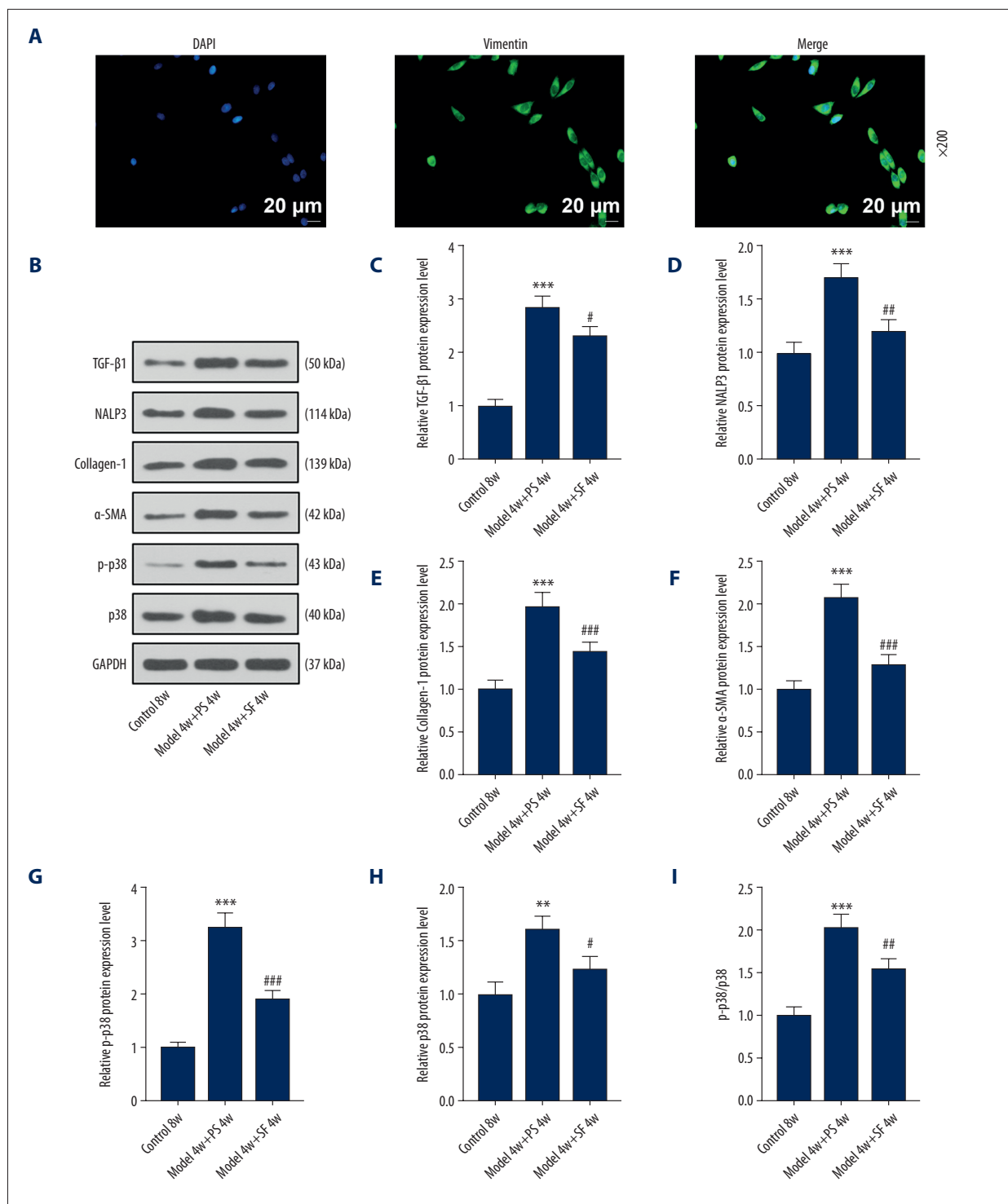
Figure 2. Fibroblasts were isolated and identified, and sodium ferulate (SF) reduced the expression of fibrosis-related proteins in silicosis mice. (**A**) Localization and expression of vimentin in cells by immunofluorescence (magnification×200, scale bars=20 μm). (**B-I**) The effect of SF on the expression of transforming growth factor-β1 (TGF-β1), neutrophil alkaline phosphatase 3 (NALP3), collagen-1, alpha-smooth muscle actin (α-SMA), phosphorylated p38 (p-p38) and p38 proteins, and the ratio of p-p38/p38 in silicosis mice was detected by western blot. Expression levels were normalized with GAPDH. All experiments were performed in triplicate and data are expressed as mean±standard deviation (SD). ** $P<0.01$, *** $P<0.001$ vs control 8 weeks; # $P<0.05$, ## $P<0.01$, ### $P<0.001$ vs model 4 weeks+physiological saline 4 weeks.

Results

Effect of SF on Lung Injury, Body Weight, Vimentin Protein, mRNA Expression, and Fibrosis in Silicosis Mice

The hematoxylin-eosin staining results showed that the Control 8w group had clear lung structures, no obvious inflammatory cell infiltration in the interstitium, and thin alveolar walls. The treatment with SF alone caused no obvious pathological damage to the lung tissue of control mice. In the lung tissues of the Model 4w+PS 4w group, significant silicosis-like cell pathological changes were observed: alveolar wall broadening, focal macrophage, and inflammatory cell infiltration (**Figure 1A**). The Model 4w+SF 4w group showed significantly inhibition of the formation and progression of silicotic nodules, and the area and number of nodules were significantly reduced compared with the Model 4w+PS 4w group (**Figure 1A**).

No significant change was observed in the weight of the mice in any group during the administration period, and the weight remained around 20-25 g (**Figure 1B**). Vimentin protein and mRNA expression were significantly increased in the Model 4w+PS 4w group compared with the Control 8w group ($P<0.001$, **Figure 1C-1E**). Vimentin protein and mRNA expression were significantly decreased in the Model 4w+SF 4w group compared with the Model 4w+PS 4w group ($P<0.001$, **Figure 1C-1E**), indicating that SF inhibited the expression of vimentin in silicosis mice, while having no effect on body weight.

As shown in **Figure 1F**, the degree of fibrosis in the Model 4w+PS 4w group was significantly increased. However, the degree of fibrosis in the Model 4w+SF 4w group was significantly reduced (**Figure 1F**), indicating that SF inhibited the lung injury and fibrosis in silicosis mice.

Cellular Immunofluorescence Detection of the Localization and Expression of Vimentin in Cells

Vimentin protein showed green fluorescence under the excitation of fluorescence microscope. DAPI staining of the nucleus was used as localization, and showed blue fluorescence, which confirmed the identity of fibroblasts for use in experiments (**Figure 2A**).

SF Reduced the High Expression of Fibrosis-Related Protein in the Lung Tissue of Model Mice

The results showed that expression of the TGF-β1, NALP3, collagen 1, α-SMA, p-p38, and p38 proteins, as well as the ratio of p-p38/p38, were significantly increased in the Model 4w+PS 4w group compared with the Control 8w group ($P<0.01$, **Figure 2B-2I**). Compared with the Model 4w+PS 4w group, TGF-β1, NALP3, collagen-1, α-SMA, p-p38, and p38 protein expression in the Model 4w+SF 4w group, as well as the ratio of p-p38/p38, were significantly decreased ($P<0.05$, **Figure 2B-2I**). The results showed that SF inhibited the expression of TGF-β1, NALP3, collagen-1, α-SMA, p-p38, and p38 proteins in silicosis mice.

Different Concentrations of SF Inhibited the Proliferation of Mouse Fibroblasts

Compared with the control group, the SF solution at various concentrations significantly inhibited the activity of pulmonary fibroblasts, and the SF solution at 0.28 mg/mL concentration had the most significant inhibitory effect ($P<0.001$, **Figure 3A**). Compared with the control group, BrdU expression (red fluorescence) in the 0.1 mg/mL and 0.28 mg/mL SF groups was significantly decreased (**Figure 3B**), indicating that SF inhibited the proliferation of pulmonary fibroblast cells.

Different Concentrations of SF Decreased the Expression of Fibrosis-Related Proteins

Compared with the control group, TGF-β1, NALP3, collagen-1, α-SMA, p-p38, and p38 proteins in the 0.1 mg/mL and 0.28 mg/mL SF groups were significantly decreased ($P<0.05$, **Figure 3C-3I**), indicating that SF inhibited the expression of TGF-β1, NALP3, collagen-1, α-SMA, p-p38, and p38 proteins in pulmonary fibroblast cells. The ratio of p-p38/p38 had the same changes ($P<0.01$, **Figure 3J**). The contents of caspase-1 and IL-1β were measured by ELISA kits. As shown in **Figure 3K and 3L**, the levels of caspase-1 and IL-1β gradually decreased as the SF concentration increased ($P<0.01$).

SRI-011381 Partially Reversed the Effect of SF on the Cell Viability

The results showed that the cell survival rate of the SF group was significantly lower than that of the control group ($P<0.001$, **Figure 4A**). Compared with the SF group, the cell survival rate of the SF+SRI-011381 group was significantly increased ($P<0.05$, **Figure 4A**). Compared with the SRI011381 group, the cell survival rate of the SF+SRI-011381 group was significantly reduced ($P<0.001$, **Figure 4A**), indicating that the proliferation of fibroblasts was promoted by SRI-011381 and inhibited by SF.

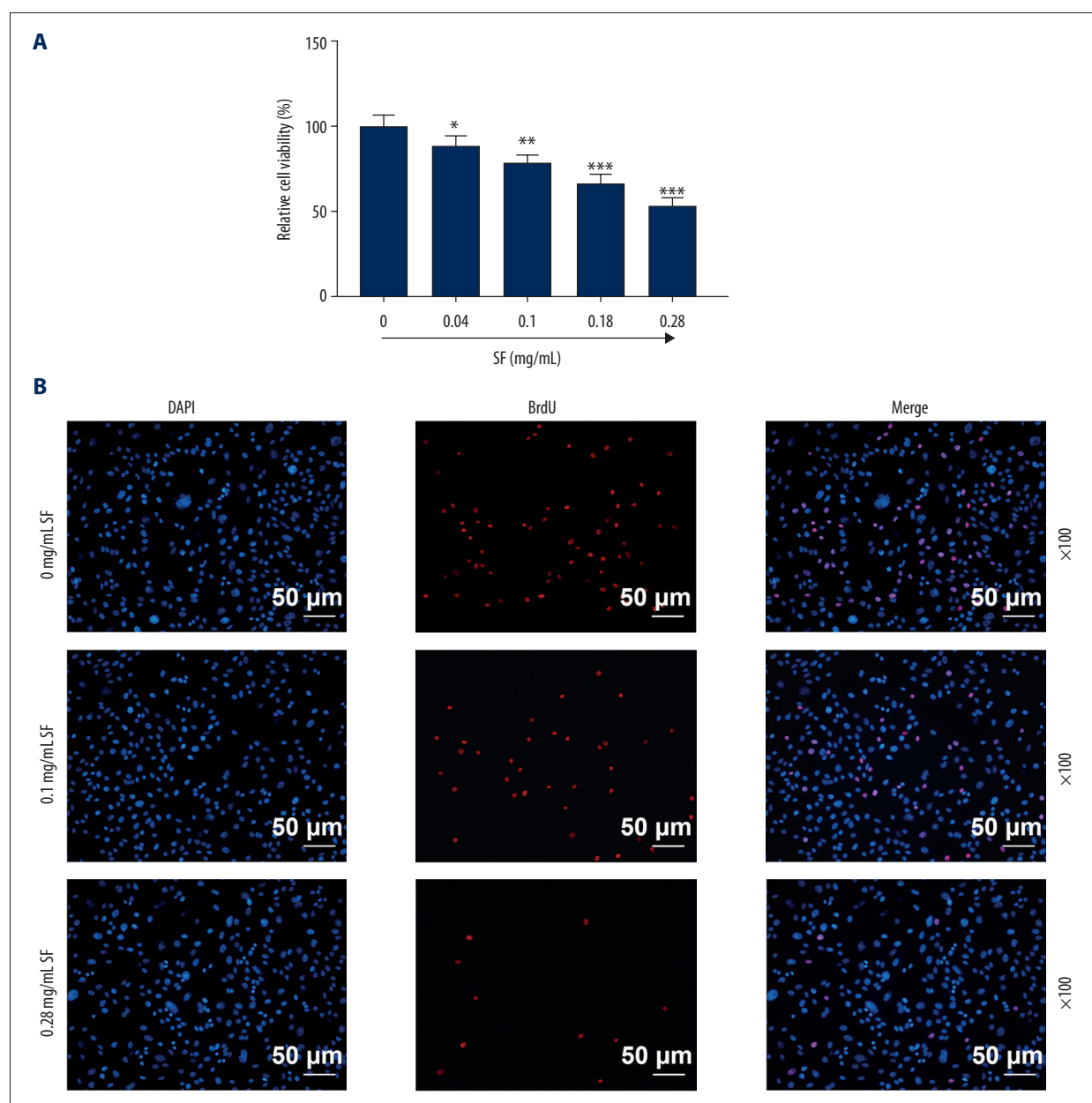### SRI-011381 Partially Reversed the Effect of SF on the Expression of Fibrosis-Related Proteins

The results showed that compared with the control group, TGF-β1, NALP3, collagen-1, and α-SMA protein expression in the SF group was significantly decreased ($P<0.001$, **Figure 4B-4F**), while TGF-β1, NALP3, collagen-1, and α-SMA expression in the SRI-011381 group was significantly increased ($P<0.05$, **Figure 4B-4F**). Compared with the SF group, the expression of

TGF-β1, NALP3, collagen-1, and α-SMA in the SF+SRI-011381 group was significantly increased (*P*<0.001, **Figure 4B-4F**). Compared with the SRI-011381 group, the expression of TGF-β1, NALP3, collagen-1, and α-SMA in the SF+SRI-011381 group was significantly decreased (*P*<0.001, **Figure 4B-4F**), indicating that SRI-011381 partially reversed the effect of SF on the expression of TGF-β1, NALP3, collagen-1, and α-SMA proteins. In addition, the decreased levels of caspase-1 and IL-1β induced by SF were partially reversed with the treatment of SRI-011381 (**Figure 4G, 4H**, *P*<0.001).

Discussion

Pneumoconiosis is a chronic progressive fibrotic interstitial pneumonia, and it represents one of the most serious occupational diseases in China [27]. In this study, the alveolar interval was significantly widened with obvious congestion and edema, and the degree of fibrosis was significantly increased in the Model 4w+PS 4w group, which was consistent with the results reported in the literature [28-31].

SF is the sodium salt of ferulate acid and the main effective component of *A. sinensis* [32]. It has been reported that ferulate acid inhibits the Smad/ILK/Snail pathway and reduces

This work is licensed under Creative Common Attribution-NonCommercial-NoDerivatives 4.0 International (CC BY-NC-ND 4.0)

e927978-8

Indexed in: [Current Contents/Clinical Medicine] [SCI Expanded] [ISI Alerting System] [ISI Journals Master List] [Index Medicus/MEDLINE] [EMBASE/Excerpta Medica] [Chemical Abstracts/CAS]
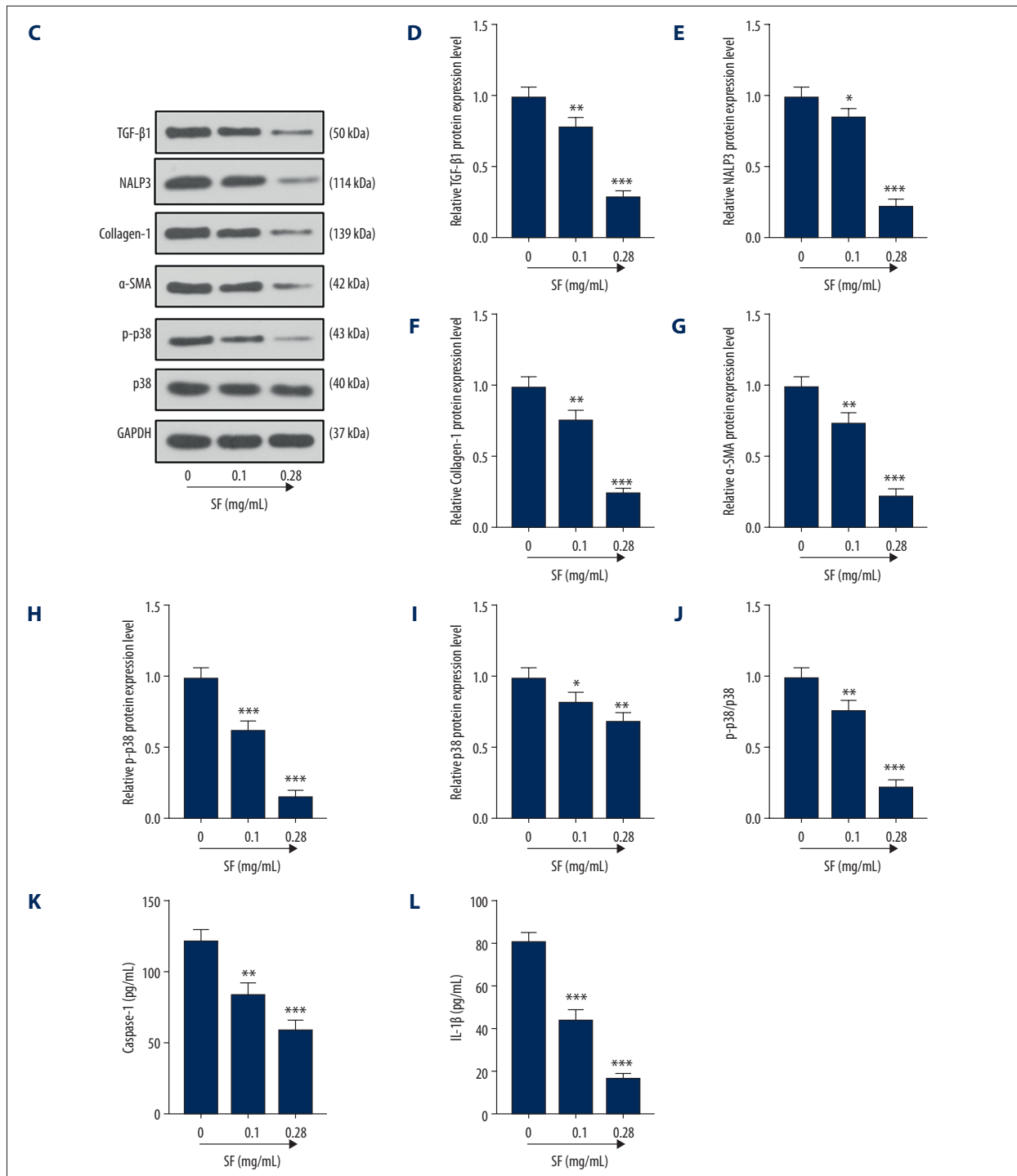
Figure 3. Sodium ferulate (SF) inhibited the proliferation of fibroblasts and the expression of transforming growth factor-β1 (TGF-β1), neutrophil alkaline phosphatase 3 (NALP3), collagen-1, alpha-smooth muscle actin (α-SMA), and phosphorylated p38 (p-p38) and p38 proteins. (**A**) The effect of SF on viability of fibroblasts was detected by Cell Counting Kit (CCK)-8 assay. (**B**) The effect of SF on proliferation of fibroblasts was observed by bromodeoxyuridine (BrdU) immunofluorescence staining (magnification×100, scale bars=50 μm). (**C-J**) The effect of SF on the expression of TGF-β1, NALP3, collagen-1, α-SMA, p-p38 and p38 proteins, and the ratio of p-p38/p38 in fibroblasts was detected by western blot. (**K, L**) The detection of caspase-1 and IL-1β levels was performed by enzyme-linked immunosorbent assay kit. Expression levels were normalized with GAPDH. All experiments were performed in triplicate, and data are expressed as mean±standard deviation (SD). * $P<0.05$, ** $P<0.01$, *** $P<0.001$ vs control group.
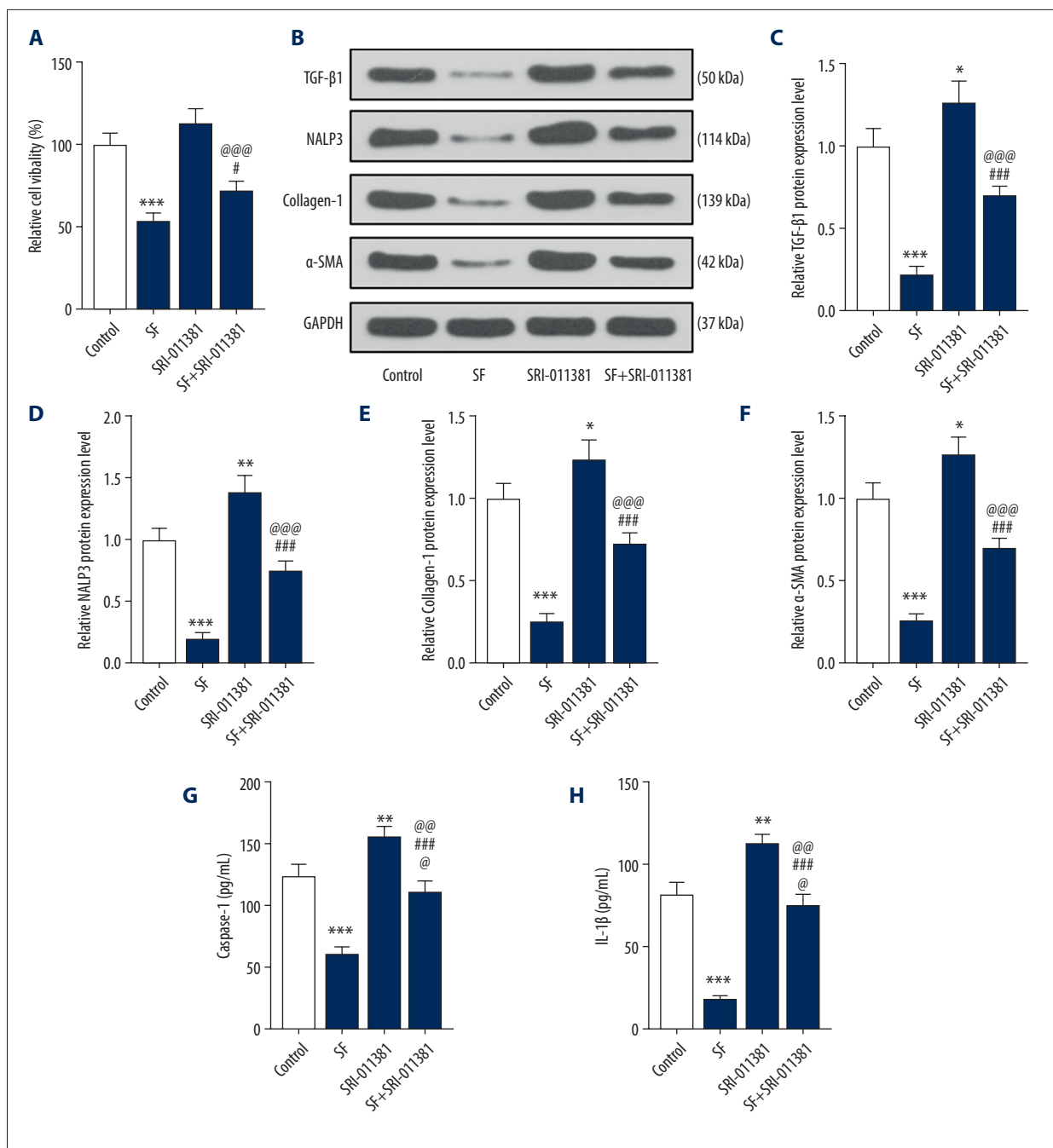
Figure 4. Transforming growth factor-β1 (TGF-β1) pathway agonists partially reversed the effect of sodium ferulate (SF) on the proliferation of fibroblasts and the expression of fibrosis-related proteins. (**A**) The effect of TGF-β pathway agonists (SRI-011381) on the viability of fibroblasts was detected by Cell Counting Kit (CCK)-8 assay. (**B-F**) The effect of SRI-011381 on the expression of TGF-β1, neutrophil alkaline phosphatase 3 (NALP3), collagen-1, and alpha-smooth muscle actin (α-SMA) proteins was detected by western blot. (**G, H**) The detection of caspase-1 and IL-1β levels was performed by enzyme-linked immunosorbent assay kit. Expression levels were normalized with GAPDH. All experiments were performed in triplicate, and data are expressed as mean±standard deviation (SD). * $P<0.05$, ** $P<0.01$, *** $P<0.001$ vs control; # $P<0.05$, ### $P<0.001$ vs SF group; @@@ $P<0.001$ vs SRI-011381 group.

TGF-β1-mediated renal tubular epithelial cells, thereby affecting renal fibrosis [33]. In this study, SF significantly improved the alveolar structure of mice, reduced the widening of the alveolar interval, decreased the inflammatory cell infiltration, and was associated with no significant fibrosis changes. These outcomes were consistent with the results reported in the literature [22].

During the formation and development of pulmonary fibrosis, many cytokine networks regulate the imbalance, resulting in the imbalance of collagen metabolism, excessive extracellular deposition, and impaired lung function [34,35]. In addition, NALP3 is abnormally activated in patients with idiopathic pulmonary fibrosis and rheumatic disease secondary pulmonary fibrosis [36, 37]. During the differentiation of cardiac fibroblasts mediated by TGF-β, the expression of IL-1β, IL-181, and caspase-1 did not change, while only the expression of NALP3 was up-regulated [38]. The activation and transformation of interstitial intrinsic fibroblasts into myofibroblasts depend on the local presence of activated TGF-β1. Myofibroblasts are characterized by stronger collagen synthesis and proliferation capacity, causing large amounts of type I and type III collagen synthesis and excessive accumulation, and increased expression of α-SMA [39]. α-SMA is a marker of activated fibroblasts, and the expression of α-SMA in the cytoplasm makes it contractile, which plays a crucial role in the process of organ fibrosis. The current study also confirmed this point [40]. NALP3, TGF-β1, and α-SMA are key fibrogenic factors, which also play a vital role in the continuous differentiation and proliferation of fibroblasts, and they may coexist in the formation of pulmonary fibrosis [41-43]. The experimental results also showed that the expression of TGF-β1, NALP3, and α-SMA in Model 4w+SF 4w group was significantly lower, while the expression of TGF-β1, NALP3, collagen-1, and α-SMA in the SRI-011381 group was significantly higher, indicating that SF affects lung fibroblasts through the NALP3/TGF-β1/α-SMA pathway. Furthermore, several studies have reported

associations with the NALP3/TGF-β1/α-SMA pathway, but the results were complicated. For example, Zhang et al [44] suggested that the NALP3 inhibitor MCC950 could ameliorate diabetes-associated kidney injury via the regulation of the expression of TGF-β1 and α-SMA. In addition, the inhibition of NLRP3 could notably rescue TGF-β1-induced myofibroblast (human dermal fibroblast) differentiation [45]. It is difficult for us to sort out the upstream and downstream relationships of the pathway based on these previous studies. Our subsequent study will focus on further understanding the underlying mechanism of SF improving pulmonary fibrosis in silicosis.

Our study suggested that SF showed protective effects against silicosis damage in vivo. Moreover, we demonstrated that SF reduced cell proliferation in lung fibroblasts by interrupting the interactions within the TGF-β1/NALP3/collagen-1/α-SMA pathway. In conclusion, our results indicate that SF could be a potential therapeutic agent for silicosis-associated pulmonary fibrosis by suppressing TGF-β1/NALP3/collagen-1/α-SMA pathway activation. Some aspects of this study could be improved. For example, although we observed the histopathological changes of model mice via hematoxylin-eosin and Masson's staining, we did not assess the O_2 saturation of model animals, which could have reflected changes in heart and lung function under pathological conditions in real time.

Conclusions

In summary, SF can effectively reduce the degree of fibrosis in the lung tissue of mice with pulmonary fibrosis. It mainly inhibits the excessive deposition of collagen fibers by inhibiting the NALP3/TGF-β1/α-SMA signaling pathway. Therefore, SF plays an important role in regulating collagen metabolism imbalance in pulmonary fibrosis and holds promise for the prevention and treatment of pulmonary fibrosis.

References:

1. Liu R, Ahmed KM, Nantajit D, et al. Therapeutic effects of alpha-lipoic acid on bleomycin-induced pulmonary fibrosis in rats. Int J Mol Med. 2007;19(6):865-73

2. Ponticos M, Holmes AM, Xu SW, et al. Pivotal role of connective tissue growth factor in lung fibrosis MAPK-dependent transcriptional activation of type I collagen. Arthritis Rheum. 2009;60(7):2142-55

3. Wang H, Mengsteab S, Tag CG, et al. Transforming growth factor-beta 1 gene polymorphisms are associated with progression of liver fibrosis in Caucasians with chronic hepatitis C infection. World J Gastroenterol. 2005;11(13):1929-36

4. Xaubet A, Marin-Arguedas A, Lario S, et al. Transforming growth factor-β1 gene polymorphisms are associated with disease progression in idiopathic pulmonary fibrosis. Am J Respir Crit Care Med. 2003;168(4):431-35

5. Razzaque MS, Taguchi T. Cellular and molecular events leading to renal tubulointerstitial fibrosis. Med Electron Microsc. 2002;35(2):68-80

6. Sun Y, Yang F, Yan J, et al. New anti-fibrotic mechanisms of n-acetyl-seryl-aspartyl-lysyl-proline in silicon dioxide-induced silicosis. Life Sci. 2010;87(7-8):232-39

7. Wang Y, Lin C, Han R, et al. Metformin attenuates TGF-β1-induced pulmonary fibrosis through inhibition of transglutaminase 2 and subsequent TGF-β pathways. 3 Biotech. 2020;10(6):287-96

8. Osborn-Heaford HL, Ryan AJ, Murthy S, et al. Mitochondrial Rac1 GTPase import and electron transfer from cytochrome C are required for pulmonary fibrosis. J Biol Chem. 2012;287(5):3301-12

9. Scotton CJ, Chambers RC. Molecular targets in pulmonary fibrosis: The myofibroblast in focus. Chest. 2007;132(4):1311-21

10. Kuang J, Xie M, Wei X. The NALP3 inflammasome is required for collagen synthesis via the NF- B pathway. Int J Mol Med. 2018;41(4):2279-87

11. Li L, Cai L, Zheng L, et al. Gefitinib inhibits bleomycin-induced pulmonary fibrosis via alleviating the oxidative damage in mice. Oxid Med Cell Longev. 2018;2018:8249693

12. Rittié L. Another dimension to the importance of the extracellular matrix in fibrosis. J Cell Commun Signal. 2015;9(1):99-100

13. Nho RS, Polunovsky V. Translational control of the fibroblast-extracellular matrix association: an application to pulmonary fibrosis. Translation (Austin). 2013;1(1):23-34

14. Liu J, Zhao B, Zhu H, et al. Wnt4 negatively regulates the TGF-β1-induced human dermal fibroblast-to-myofibroblast transition via targeting Smad3 and ERK. Cell Tissue Res. 2020;379(3):537-48

15. Mao MU, Cheng D, Chen Y, et al. [Preventive effect of sodium ferulate on pulmonary fibrosis in rats.] J Guiyang Med Coll. 2010;035(003): 251-54 [in Chinese]

16. Zhao P, Zhou WC, Li DL, et al. Total glucosides of Danggui Buxue Tang attenuate BLM-induced pulmonary fibrosis via regulating oxidative stress by inhibiting NOX4. Oxid Med Cell Longev. 2015;8(11):645-57

17. Gao J, Feng LJ, Huang Y, et al. Total glucosides of Danggui Buxue Tang attenuates bleomycin-induced pulmonary fibrosis via inhibition of extracellular matrix remodelling. J Pharm Pharmacol. 2012;64(6):811-20

18. Li-xia W, Feng W, Xin C, et al. Pharmacological research progress of sodium ferulate in cardio-cerebral vascular disease. Chinese Medicinal Herb. 2019;50(3):235-40

19. Li FQ, Hua S, Xu C, et al. Mannose 6 phosphate modified bovine serum albumin nanoparticles for controlled and targeted delivery of sodium ferulate for treatment of hepatic fibrosis. J Pharm Pharmacol. 2009;61(9):1155-61

20. Shokeir AA, Hussein AA, Soliman SA, et al. Recoverability of renal functions after relief of partial ureteric obstruction of solitary kidney: Impact of ferulic acid. BJU Int. 2012;110(6):904-11

21. Wang X, Zhang Y, Zhang W, et al. MCPIP1 regulates alveolar macrophage apoptosis and pulmonary fibroblast activation after in vitro exposure to silica. Toxicol Sci. 2016;151(1):126-38

22. Kuang J, Wei XL, Xie M. [The effect of sodium ferulate in experimental pulmonary fibrosis via NALP3 inflammasome.] Sichuan Da Xue Xue Bao Yi Xue Ban. 2017;48(4):503-8 [in Chinese]

23. Zhang M, Qian C, Zheng ZG, et al. Jujuboside A promotes Aβ clearance and ameliorates cognitive deficiency in Alzheimer's disease through activating Axl/HSP90/PPARγ pathway. Theranostics. 2018;8(15):4262-78

24. Hu L, Pu Q, Zhang Y, et al. Expansion and maintenance of primary corneal epithelial stem/progenitor cells by inhibition of TGFβ receptor I-mediated signaling. Exp Eye Res. 2019;182:44-56

25. Li-jun F, Lin-mao L, Wei Z. Effects of Osthol on TGF-β1-induced proliferation and collagen synthesis of pulmonary fibroblasts. China J Tradit Chin Med and Pharm. 2017;34(05):95-99

26. Lyu L, Wang H, Li B, et al. A critical role of cardiac fibroblast-derived exosomes in activating renin angiotensin system in cardiomyocytes. J Mol Cell Cardiol. 2015;89(13):268-79

27. Zhao H, Wang Y, Qiu T, et al. Autophagy, an important therapeutic target for pulmonary fibrosis diseases. Clin Chim Acta. 2020;502(34):139-47

28. Cassel SL, Eisenbarth SC, Iyer SS, et al. The Nalp3 inflammasome is essential for the development of silicosis. Proc Natl Acad Sci USA. 2008;105(26):9035-40

29. Dong Z, Zhao X, Tai W, et al. IL-27 attenuates the TGF-β1-induced proliferation, differentiation and collagen synthesis in lung fibroblasts. Life Sci. 2016;146(51):24-33

30. Yang M, Qian X, Wang N, et al. Inhibition of MARCO ameliorates silica-induced pulmonary fibrosis by regulating epithelial-mesenchymal transition. Toxicol Lett. 2019;301(58):64-72

31. Deng H, Xu H, Zhang X, et al. Protective effect of Ac-SDKP on alveolar epithelial cells through inhibition of EMT via TGF-β1/ROCK1 pathway in silicosis in rat. Toxicol Appl Pharmacol. 2016;294(35):1-10

32. De H, Zhi-liang Z, Jian-hua C, et al. Sodium ferulate against liver fibrosis in rats. World Chin J Digesto. 2006;10(2):240-41

33. Wei MG, Sun W, He WM, et al. Ferulic acid attenuates TGF-β1-induced renal cellular fibrosis in NRK-52E cells by inhibiting Smad/ILK/Snail pathway. Evid Based Complement Alternat Med. 2015;49(10):619720

34. Lee SY, Cho SS, Bae CS, et al. Socheongryongtang suppresses COPD-related changes in the pulmonary system through both cytokines and chemokines in a LPS COPD model. Pharm Biol. 2020;58(1):538-44

35. Helal MG, Said E. Carvedilol attenuates experimentally induced silicosis in rats via modulation of P-AKT/mTOR/TGFβ1 signaling. Int Immunopharmacol. 2019;70(9):47-55

36. Lasithiotaki I, Giannarakis I, Tsitoura E, et al. NLRP3 inflammasome expression in idiopathic pulmonary fibrosis and rheumatoid lung. Eur Respir J. 2016;47(3):910-18

37. Artlett CM, Sassi-Gaha S, Rieger JL, et al. The inflammasome activating caspase 1 mediates fibrosis and myofibroblast differentiation in systemic sclerosis. Arthritis Rheum. 2011;63(11):3563-74

38. Bracey NA, Gershkovich B, Chun J, et al. Mitochondrial NLRP3 protein induces reactive oxygen species to promote Smad protein signaling and fibrosis independent from the inflammasome. J Biol Chem. 2014;289(28):19571-84

39. Pechkovsky DV, Prêle CM, Wong J, et al. STAT3-mediated signaling dysregulates lung fibroblast-myofibroblast activation and differentiation in UIP/IPF. Am J Pathol. 2012;180(4):1398-412

40. Li J, Yao W, Hou JY, et al. Crystalline silica promotes rat fibrocyte differentiation in vitro, and fibrocytes participate in silicosis in vivo. Biomed Environ Sci. 2017;30(9):649-60

41. Yang X, Xuemei MA, Sun Y, et al. The expression and significance of serum IL-27 and TGF-β1 in patients with pulmonary fibrosis. China Modern Doctor. 2015;53(13):13-17

42. Liang Y, Jiang L, Qin W, et al. Serum IL-13, TGF-β1, IL-8 levels in idiopathic pulmonary fibrosis and correlation with lung function. China Modern Doctor. 2015;53(11):1-3

43. Shu-ning Z, Yan Q, Zhi-qiao H, et al. Effect of ursolic acid on the number of alveolar macrophage and expression of vimentin in silicotic rats. China Occupat Med. 2018;45(5):572-80

44. Liu Z, Zhou Y, Liang G, et al. Circular RNA hsa_circ_001783 regulates breast cancer progression via sponging miR-200c-3p. Cell Death Dis. 2019;10(2):55

45. Pinar AA, Yuferov A, Gaspari TA, et al. Relaxin can mediate its anti-fibrotic effects by targeting the myofibroblast NLRP3 inflammasome at the level of caspase-1. Front Pharmacol. 2020;11:1201

This work is licensed under Creative Common Attribution-NonCommercial-NoDerivatives 4.0 International (CC BY-NC-ND 4.0)

e927978-12

Indexed in: [Current Contents/Clinical Medicine] [SCI Expanded] [ISI Alerting System] [ISI Journals Master List] [Index Medicus/MEDLINE] [EMBASE/Excerpta Medica] [Chemical Abstracts/CAS]